

An examination of the differences between surface and free-air temperature trend at high-elevation sites: Relationships with cloud cover, snow cover, and wind

N. C. Pepin¹

Department of Geography, University of Portsmouth, Hants, UK

J. R. Norris

Scripps Institution of Oceanography, La Jolla, California, USA

Received 29 April 2005; revised 12 August 2005; accepted 29 September 2005; published 24 December 2005.

[1] Contrasts in high-elevation surface and free-tropospheric temperatures between 1971 and 1996 are examined by comparing surface temperatures from a subset of 72 stations in the GHCN (Global Historical Climate Network) and CRU (Climatic Research Unit) homogeneity adjusted surface data sets with free-air temperatures interpolated to the same locations from NCEP/NCAR Reanalysis R1. The selected stations are above the mean elevation of the surrounding topography, often located on mountain summits. Surface temperatures, free-air temperatures, and their difference (ΔT) are found to be related to independent surface cloud observations from the NDP-026C archive, local wind speed, satellite records of snow cover (NSIDC), and reanalysis wind components. Significant correlations are observed at most stations, and correlation spatial patterns are consistent for different subperiods of the record (e.g., presatellite era versus satellite era). Stepwise regression models built to predict surface temperatures, free-air temperatures, and ΔT from the above meteorological parameters typically explain 20–40% of the temperature variability on an annual basis and more for individual seasons. The stationarity of relationships between temperature and snow/cloud/wind is examined by comparing the temporal trends in the original temperatures with predicted trends from the best fit regression model and trends in model residuals. This provides an assessment of how much of any ΔT trends can be accounted for by changes in meteorology. Significant daytime ΔT residual trends occur primarily in Turkey and eastern China, but significant nighttime ΔT residual trends are more geographically widespread. While daytime residual trends may be the result of surface radiative cooling by increasing anthropogenic aerosol, attribution of nighttime residual trends is uncertain.

Citation: Pepin, N. C., and J. R. Norris (2005), An examination of the differences between surface and free-air temperature trend at high-elevation sites: Relationships with cloud cover, snow cover, and wind, *J. Geophys. Res.*, 110, D24112, doi:10.1029/2005JD006150.

1. Introduction

[2] Numerous recent studies have found contrasting trends in surface and free-air tropospheric temperatures over the past 2 to 3 decades, typically with more warming at the surface than in the free troposphere. Although most investigations have been concerned with temperature trends on the global scale [*National Research Council, 2000; Christy et al., 2003; Lanzante et al., 2003; Jones and Moberg, 2003; Fu et al., 2004*], differing trends in surface and tropospheric temperature have also been noted on a regional and local basis [*Seidel and Free, 2003; Pepin*

and Losleben, 2002; Pepin and Seidel, 2005]. Interpretation of such differences is complex, and it is currently uncertain whether the contrasting trends indicate a real long-term shift in the state of the climate system or merely result from inadequacies in and incompatibilities between the various observing systems involved, which include surface instruments, radiosondes and satellites.

[3] One difficulty with assessing potential errors in surface and tropospheric temperature data is that the measurements are not made at the same elevation. The present study overcomes this limitation by comparing high-elevation screen-level surface temperature observations (T_s) with free-air tropospheric data interpolated to the same location and elevation (T_a). Surface temperatures are obtained from a selection of high-elevation stations within the Global Historical Climate Network (GHCN) and Climate Research Unit (CRU) data sets with homog-

¹Also at NOAA Air Resources Laboratory, Silver Spring, Maryland, USA.

Table 1. List of 72 Stations^a

WMO Number	Name	Latitude	Longitude	Elevation, m	Topographical Class	Effective Sample Size
68624	Fraserburg	-31.92	21.52	1300	3	1.00
50727	Arxan	47.17	119.95	1028	1	0.15
51156	Hoboksar	46.78	85.72	1294	6	0.07
51288	Baytik-Shan	45.37	90.53	1651	3	0.07
51467	Balguntay	42.67	86.33	1753	6	0.07
52118	Yiwu	43.27	94.7	1729	1	0.07
52495	Bayan-Mod	40.75	104.5	1329	6	0.07
52602	Lenghu	38.83	93.38	2734	1	0.07
52713	Da-Qaidam	37.85	95.37	3174	2	0.07
52787	Wushaoiling	37.2	102.87	3044	6	0.07
52996	Huajialing	35.38	105	2450	6	0.07
53149	Mandal	42.53	110.13	1223	3	0.07
53231	Hails	41.45	106.38	1510	1	0.07
53352	Darhan-Muminggan	41.7	110.43	1376	4	0.07
53391	Huade	41.9	114	1484	2	0.07
53480	Jining	41.03	113.07	1416	3	0.07
53543	Dongsheng	39.83	109.98	1459	1	0.07
53588	Wutai-Shan	39.03	113.53	2898	1	0.07
53787	Yushe	37.07	112.98	1042	5	0.07
53923	Xifengzhen	35.73	107.63	1423	1	0.07
54012	Xi-Ujimqin-Qi	44.58	117.6	997	3	0.07
54208	Duolun	42.18	116.47	1247	3	0.07
54311	Weichang	41.93	117.75	844	5	0.07
54826	Tai-Shan	36.25	117.1	1536	1	0.07
56079	Ruo'ergai	33.58	102.97	3441	6	0.07
56152	Sertar	32.28	100.33	3896	5	0.15
56182	Songpan	32.65	103.57	2852	5	0.07
56257	Litang	30	100.27	3950	2	0.15
56357	Daocheng	29.05	100.3	3729	3	0.15
56385	Emei-Shan	29.52	103.33	3049	1	0.07
56586	Zhaotong	27.33	103.75	1950	5	0.07
56684	Huize	26.42	103.28	2110	3	0.07
56691	Weining	26.87	104.28	2236	1	0.07
56778	Kunming	25.02	102.68	1892	2	0.07
56786	Zhanyi	25.58	103.83	1900	6	0.07
57046	Hua-Shan	34.48	110.08	2063	1	0.07
57707	Bijie	27.3	105.23	1511	3	0.07
57776	Nanyue	27.3	112.7	1268	1	0.07
57902	Xingren	25.43	105.18	1379	1	0.07
57922	Dushan	25.83	107.55	971	1	0.07
58437	Huang-Shan	30.13	118.15	1836	1	0.07
58445	Tainmu-Shan	30.35	119.42	1494	1	0.07
58506	Lu-Shan	29.58	115.98	1165	6	0.07
58931	Jiuxian-Shan	25.72	118.1	1651	1	0.07
59007	Guangnan	24.07	105.07	1251	2	0.07
47618	Matsumoto	36.25	137.97	611	5	0.20
35394	Karaganda	49.8	73.13	555	3	0.20
30393	Cul'man	56.83	124.87	858	3	0.50
31004	Aldan	58.62	125.37	682	2	0.50
38696	Samarkand	39.57	66.95	724	4	0.20
71092	Dewar-Lakes	68.65	-71.17	527	5	1.00
71870	Swift-Current	50.28	-107.68	818	5	0.80
72564	Cheyenne	41.15	-104.82	1872	3	0.80
94326	Alice-Springs	-23.8	133.88	547	3	1.00
13353	Sarajevo	43.82	18.33	511	5	0.25
16040	Tarvisio	46.5	13.58	778	5	0.25
16179	Frontone	43.52	12.73	574	1	0.25
16252	Campobasso	41.57	14.65	807	1	0.25
12510	Sniezka	50.73	15.73	1613	1	0.25
12625	Zakopane	49.3	19.95	860	5	0.25
12650	Kasprowy-Weir	49.23	19.98	1989	1	0.25
17084	Corum	40.55	34.97	776	5	0.15
17090	Sivas	39.75	37.02	1285	5	0.15
17092	Erzincan	39.73	39.5	1215	5	0.15
17096	Erzurum	39.92	41.27	1758	2	0.15
17128	Ankara	40.12	32.98	949	5	0.15
17170	Van	38.45	43.32	1661	3	0.15
17188	Usak	38.67	29.42	919	6	0.15
17190	Afyon	38.75	30.53	1034	3	0.15
17240	Isparta	37.75	30.55	997	5	0.15
17260	Gaziantep	37.08	37.37	855	1	0.15
17292	Mugla	37.2	28.35	646	1	0.15

^aLatitude and longitude are in decimal degrees. Topographical class is discussed in the main text: 1, summit or ridge; 2, slope; 3, flat; 4, basin; 5, incised valley; 6, not enough information.

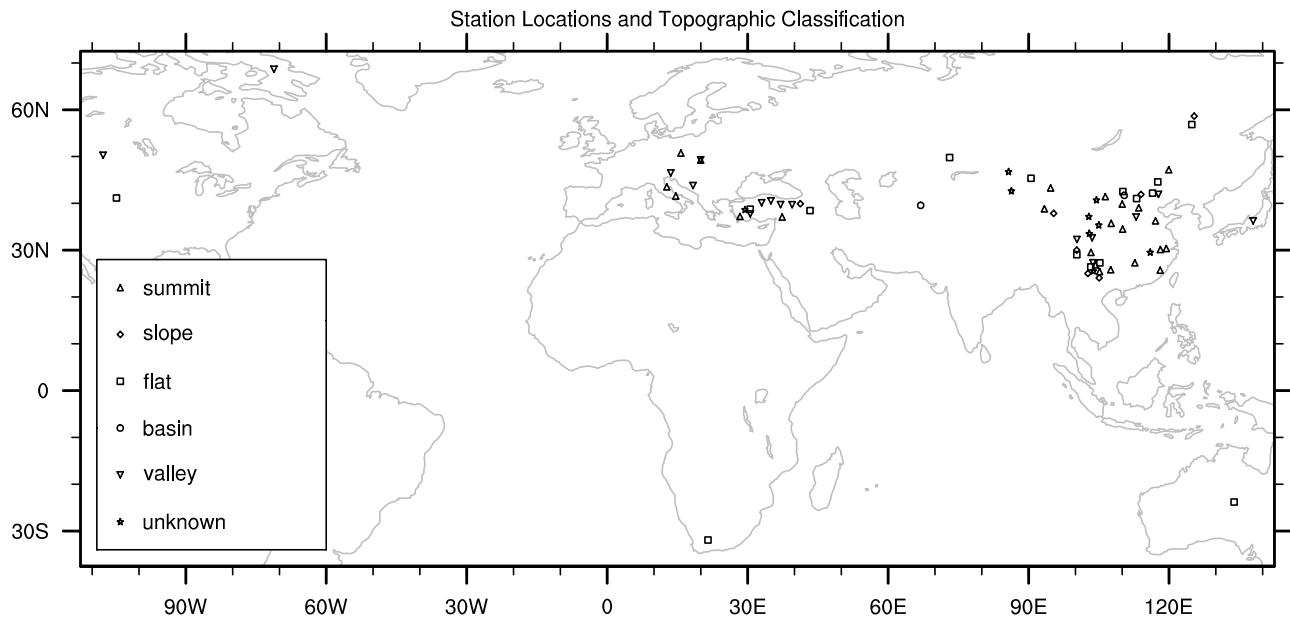


Figure 1. Geographical distribution of the 72 GHCN and CRU stations used in this study with symbols indicating site topography: summit or ridge (upward pointing triangle), slope (diamond), flat (square), basin (circle), incised valley (downward pointing triangle), and unknown (star).

enous records (mostly in the Northern Hemisphere), and interpolated free-air temperatures are obtained from the NCAR/NCEP reanalysis R1. Since surface properties and atmospheric processes can have different effects on T_s and T_a , it is possible that changes in meteorological conditions may be partly responsible for contrasting trends in surface and free-air temperature.

[4] Time series of T_s , T_a , and their difference ($T_s - T_a$, referred to as ΔT) are examined for relationships to other meteorological parameters including cloud cover, zonal and meridional wind components, surface wind speed, and snow cover. Strong relationships with these parameters, especially as measured by independent data, would increase confidence that at least some of the difference in trends observed between the surface and free-air data sets is real, rather than solely an artefact of data error. Furthermore, it is of interest whether relationships between ΔT and meteorological parameters are consistent over long periods of time (i.e., stationary). If so, any secular trends in ΔT should be accompanied by attendant changes in cloud, wind, or snow.

[5] In section 2, expected relationships between ΔT and other meteorological parameters are reviewed through discussion of previous literature. Section 3 introduces the data sets and preparation methods. Individual relationships are discussed in section 4, leading to regression models to predict surface, free-air temperatures, and ΔT . Section 5 examines temporal trends in temperatures (including ΔT) and discusses the extent to which cloud, wind, and snow changes are associated with the observed temperature changes.

2. Controls of ΔT

[6] Numerous field studies have examined instantaneous and climatological mean differences between surface (screen level) temperatures, usually measured on mountain

summits, and temperatures in the free air nearby at equivalent elevations measured from radiosondes [Samson, 1965; McCutchan, 1983; Richner and Phillips, 1984; Tabony, 1985]. Barry [1992] provides a summary of such studies. The main temporal controls of the difference (ΔT) are cloudiness, advection (winds), snow cover, and topographical characteristics.

[7] Diurnal and seasonal structures in the differences are frequently reported, with mountain top sites in extratropical latitudes tending to be warmer than the free air ($\Delta T > 0$) in the midday period and in summer, but colder ($\Delta T < 0$) at night and in winter [McCutchan, 1983; Richner and Phillips, 1984]. This suggests that net local surface radiation flux is an important control. Cloud cover acts to suppress differences in surface and free air temperature by reducing the otherwise enhanced surface heating during day and enhanced surface cooling during night. Thus daytime positive values of ΔT ($T_s > T_a$) are reduced under increased cloudiness, while nighttime negative values are minimized. Low clouds are more influential than high clouds at night since low clouds are warmer and consequently emit more thermal radiation toward the surface. Moisture, in the form of specific humidity, controls latent heat transfer. In a dry atmosphere where evaporation is limited, free air temperatures aloft are likely to be relatively cold in comparison with the mountain surface [Molnar and Emanuel, 1999].

[8] Surface temperature often lags behind free-air temperature in cases of strong large-scale advection, particularly in sheltered locales such as valley bottoms. This means ΔT will be negative ($T_s < T_a$) for warm advection and positive for cold advection ($T_s > T_a$). Advection is closely related to the direction of the large-scale wind and is of particular importance in midlatitudes where air mass contrasts are great. To our knowledge no systematic investigation of this phenomenon has been published.

Table 2. Correlations Between Total and Low Cloud Cover Anomalies and Temperature Anomalies (T_s , T_a and ΔT)^a

	Surface		Free Air		Delta-T	
	Max	Min	Max	Min	Max	Min
Mean correlation	-0.281	0.079	-0.207	-0.065	-0.248	0.179
Median correlation	-0.307	0.070	-0.238	-0.040	-0.211	0.173
Mean (abs value)	0.284	0.156	0.224	0.110	0.261	0.218
Max correlation (+ve)	0.086	0.387	0.315	0.187	0.144	0.543
Min correlation (-ve)	-0.740	-0.435	-0.564	-0.432	-0.714	-0.299
Number sig., ^b %	79.5	56.7	75.2	38.9	81.8	65.8
Number m.sig., ^c %	0	2.8	2.8	8.8	2.2	3.2
Sig. +ve, %	0	43.8	1.7	6.1	1.2	60.6
Sig. -ve, %	79.5	12.9	73.5	32.8	80.6	5.2
Total -, %	96.2	35.5	86.9	60.5	89.8	26.5
Mean cor. (low cloud)	-0.264	0.070	-0.190	-0.074	-0.243	0.180
Median (low cloud)	-0.331	0.063	-0.222	-0.071	-0.216	0.174

^aThe majority of the table concerns total cloud, with low cloud correlations limited to the bottom two lines. All derived correlations in this table and Tables 3–7 (means, medians and percentages) take spatial autocorrelation into account by weighting individual station values by their relative effective sample size (see text). In this table and all subsequent tables.

^bSig. means $p < 0.05$ (significant).

^cM.sig. means $p < 0.10$ (marginally significant).

[9] Snow cover suppresses surface heating by acting as a heat sink, in that energy is transferred to the atmosphere in the melting process and the sensible heat flux is greatly reduced. This, combined with the high surface albedo, will make ΔT negative in most snow-covered areas, even by day.

[10] Absolute elevation is also important [Molnar and Emanuel, 1999], and mean annual values of ΔT become more positive at higher elevations, assuming radiative and convective equilibrium.

[11] The topography at a particular locale can modify the relationships described above in complex ways. A mountain peak or summit site will be more strongly influenced by free-air advection than a valley site, so values of ΔT should be less temporally variable and closer to zero at these exposed locations. However, it is not clear whether the above relationships between ΔT , wind speed, cloud and snow become more or less influential at summit sites.

3. Data and Preparation Methods

[12] Although free-air temperatures and snow cover were available worldwide from global gridded data sets, availability of both simultaneous homogenous surface temperature records and high-resolution station cloud cover reports placed limits on possible locations for study. Since our research focuses on examining the factors responsible for past surface and free-air temperature differences rather than presenting a comprehensive global analysis of observed trends, data quality was of more importance than quantity (length of period, spatial coverage). Only 228 high-elevation (>500 m) GHCN/CRU surface temperature stations, mostly in the Northern Hemisphere, also had cloud cover data. Many of these stations were in areas of complex topography and did not have elevations greater than the average elevation of the surrounding terrain. Because it is important that the interpolated reanalysis free-air temperature represent true free-air conditions rather than an extrapolation below the Earth's surface, a subset of 72 stations with elevations well above the mean elevation of the four surrounding $2.5^\circ \times 2.5^\circ$ reanalysis grid points was chosen for analysis (Table 1 and Figure 1). The plurality of these stations is exposed mountain summit sites, but there are a few sites

in high-elevation basins or valleys. Sites are distributed over most of the major continents, but with a heavy concentration in Eurasia. The network does not sample the Southern Hemisphere well (only two sites), and South America is omitted. A variety of elevations (from 500 m to 3950 m) are sampled, with 7 sites located at greater than 3000 m. The mean station elevation is 1554 m. The 1971–1996 time period is analyzed because this is when reliable cloud and temperature data are both available. The trend analysis (section 5) is restricted to 1971–1990 because of data gaps in the 1990s at some stations.

3.1. Temperature

[13] Surface temperatures in the form of monthly mean maximum and minimum temperature anomalies were calculated for the 72 sites from the GHCN version 2 and CRU data sets [Peterson and Vose, 1997; Peterson et al., 1998; Jones, 1994; Jones et al., 1999; Jones and Moberg, 2003]. These data sets have been adjusted to improve temporal homogeneity and are frequently used in climate change studies.

[14] Free-air temperatures from the NCEP/NCAR reanalysis R1 [Kistler et al., 2001] were interpolated both vertically and horizontally to the exact location of the surface site using one or two of the four times daily grids (0, 6, 12 and 18 UTC). To ensure fair comparison with surface maxima and minima, grids corresponding to a time between 1230–1530 local solar time LST (maxima) and 0430–0730 LST (minima) at each longitude were used. Where necessary, temporal interpolation to a 3 hourly reading (i.e., midway between 6 hourly values) was obtained via simple averaging of the two relevant grids. Spatial interpolation was linear, with the vertical interpolation to the relevant height at the four nearest grid points done first. Interpolated temperatures are derived from aboveground pressure level data for the two levels immediately above and below the elevation of the surface site, not skin temperatures produced by the model [see Kalnay and Cai, 2003; Trenberth, 2004; Vose et al., 2004]. Because the surface sites are above the surrounding reanalysis grid points, local boundary layer effects, which would invalidate the linear assumption, are minimized. Since the reanalysis assimilated a mix of satellite and radiosonde

Table 3. Correlations Between u Wind Component Anomaly and Temperature Anomalies

	Surface		Free Air		Delta-T	
	Max	Min	Max	Min	Max	Min
Mean correlation	0.083	0.054	0.046	0.059	0.136	0.037
Median correlation	0.089	0.103	0.078	0.143	0.137	0.047
Mean (abs value)	0.213	0.235	0.212	0.225	0.184	0.144
Max correlation (+ve)	0.535	0.531	0.583	0.539	0.597	0.317
Min correlation (–ve)	–0.422	–0.499	–0.475	–0.482	–0.414	–0.558
Number sig., ^a %	70.6	72.9	62.6	75.9	60.3	40.0
Number m.sig., ^b %	4.0	1.7	12.8	2.2	5.5	1.9
Sig. +ve, %	47.4	46.1	39.8	51.3	52.8	24.9
Sig. –ve, %	23.2	26.8	22.8	24.6	7.5	15.1
Total –, %	30.1	35.1	34.2	33.2	22.5	34.8

^aSig. means $p < 0.05$ (significant).

^bM.sig. means $p < 0.10$ (marginally significant).

observations but no surface observations, T_a and T_s come from independent sources. Despite the incorporation of a GCM in the reanalysis, tropospheric temperatures are highly dependent on the observations over the well-sampled Northern Hemisphere continents. Ease of interpolation to the station locations was the main reason free-air temperatures were obtained from the reanalysis rather than the original observations (radiosonde and satellite combination), and we must be cautious in our interpretation of the results (see final discussion). The known snow cover error in R1 does not impact the above surface temperatures used in this study (see *Kanamitsu et al.* [2002] for further discussion), but general concerns remain [*Chelliah and Ropelewski*, 2000].

[15] Monthly ΔT values were calculated by subtracting the mean free-air temperature from the mean surface temperature ($T_s - T_a$) for each month (day and night separately). These were then converted into anomalies with respect to month. Daytime and nighttime values of ΔT are often referred to as ΔT max and ΔT min respectively.

3.2. Cloud Cover

[16] Observations of sky cover by all clouds (total cloud cover) and by only low clouds (low cloud cover) were taken from 3-hourly surface synoptic reports collected in the NDP-026C archive [*Hahn and Warren*, 1999]. Since many of the cloud cover/temperature relationships are strongly dependent on time of day, only those observations closest to the times of day of maximum and minimum temperature were used (1230–1530 LST and 0430–0730 LST, respectively). These observations were averaged to monthly mean

values of total and low cloud cover (day and night separately) and then converted to anomalies with respect to month. Because surface observers have difficulty visually detecting clouds on dark nights, only those observations made under conditions of sufficient lunar illumination according to the criterion of *Hahn et al.* [1995] were averaged. Although individual 3-hourly cloud cover values are not normally distributed, the monthly anomalies are close to normally distributed.

3.3. Snow Cover

[17] Snow cover for each month was assessed from the National Snow and Ice Data Center (NSIDC) Equal Area Scalable Earth (EASE) gridded weekly version 2 data set [*Armstrong and Brodzik*, 2002], which indicates for each week from 1971 to 1996 presence or absence of snow cover on a 25 km equal-area grid (Lambert's equal area azimuthal projection: <http://nsidc.org/data/ease/>). The relevant grid pixel was identified for each station, and a snow index approximating the percentage of time with snow cover was calculated for each month by assigning 1 to snow-covered weeks and 0 to snow-free weeks and averaging the 4 or 5 weekly values. Individual weeks were assigned to the month with the most days in that week (e.g., week of 29 January to 4 February would be assigned to February). There are limitations to comparing a station point measurement (cloud, wind and temperature) with a pixel value (snow), especially at the edge of the global snow cover extent, and in areas of extreme relief (where there could be a systematic bias depending on the relative elevation of the station and the majority of the pixel area). However, these

Table 4. Correlations Between v Wind Component Anomaly and Temperature Anomalies

	Surface		Free Air		Delta-T	
	Max	Min	Max	Min	Max	Min
Mean correlation	0.185	0.301	0.265	0.327	–0.086	–0.013
Median correlation	0.203	0.291	0.279	0.315	–0.128	–0.030
Mean (abs value)	0.222	0.306	0.265	0.327	0.189	0.150
Max correlation (+ve)	0.536	0.623	0.550	0.630	0.438	0.457
Min correlation (–ve)	–0.366	–0.321	–0.013	0.025	–0.599	–0.555
Number sig., ^a %	69.9	80.7	84.5	97.8	62.8	43.5
Number m.sig., ^b %	4.9	2.2	1.7	0.5	7.8	4.2
Sig. +ve, %	66.0	80.2	84.5	97.8	12.6	19.7
Sig. –ve, %	3.9	0.5	0	0	50.2	23.8
Total –, %	15.7	3.4	0.5	0	64.5	50.7

^aSig. means $p < 0.05$ (significant).

^bM.sig. means $p < 0.10$ (marginally significant).

Table 5. Correlations Between Station Wind Speed Anomaly and Temperature Anomalies

	Surface		Free Air		Delta-T	
	Max	Min	Max	Min	Max	Min
Mean correlation	0.044	0.063	-0.010	0.006	0.108	0.078
Median correlation	0.020	0.048	-0.043	0.012	0.116	0.101
Mean (abs value)	0.100	0.114	0.108	0.083	0.145	0.138
Max correlation (+ve)	0.413	0.372	0.342	0.202	0.397	0.419
Min correlation (-ve)	-0.266	-0.231	-0.312	-0.239	-0.587	-0.339
Number sig. ^a %	25.8	30.4	40.3	36.1	57.8	42.8
Number m.sig. ^b %	13.2	2.2	3.3	2.8	2.2	5.0
Sig. +ve, %	17.0	26.5	19.7	20.1	53.2	35.4
Sig. -ve, %	8.8	3.9	20.6	16.0	4.6	7.4
Total -, %	38.1	29.2	60.3	41.5	19.9	28.2

^aSig. means $p < 0.05$ (significant).

^bM.sig. means $p < 0.10$ (marginally significant).

potential discrepancies are minor and have limited influence on snow index anomalies at any one location.

3.4. Horizontal Wind Components and Wind Speed

3.4.1. Regional

[18] Zonal (u) and meridional (v) wind components (ms^{-1}) were extracted from the NCEP/NCAR reanalysis mean monthly files and interpolated vertically and horizontally to station locations in the same way as were free-air temperatures. The derived components are representative of the synoptic-scale gradient wind and not the local surface wind at the surface site, which will be influenced by topographical effects. Such winds are therefore used to represent large-scale air mass advection. The sign of the v component in the Southern Hemisphere was reversed such that positive/negative flow is poleward/equatorward (northerly/southerly flow).

3.4.2. Station Specific Wind Speed

[19] Wind speed recorded at the synoptic station was also available in the NDP-026C archive [Hahn and Warren, 1999]. Local surface wind speed can be substantially different from that derived from the regional wind components, especially at sheltered locations or in areas of complex topography.

3.5. Analyses

[20] All parameters were converted to anomalies. Correlations between monthly anomalies in surface, free-air temperatures, ΔT , and cloud, wind, and snow were examined for all sites. Stepwise regression models were derived for surface, free-air, and ΔT temperature anomalies for all

72 sites on the basis of cloud, wind, and snow anomalies. Although correlations and models were calculated for individual meteorological seasons (DJF, MAM, JJA, SON), for reasons of space the figures and tables mostly show results calculated over the whole year. Trends in actual temperature anomalies (1971–1990) were compared to those predicted by the best regression model based on cloud, wind, and snow anomalies at each site, and to trends in the residual differences between actual and predicted temperature anomalies. In this way the stationarity of locally relevant cloud, wind, and snow versus temperature relationships can be examined.

[21] Because trends were not removed from temperature and meteorological parameters before calculating model regression coefficients, the predicted trends are not entirely independent from the observed trends. This has little impact on our analyses, however, since correlations and coefficients based on detrended data are nearly the same as those for nondetrended data (not shown).

[22] As can be seen in Figure 1, the distribution and density of stations is highly nonuniform. Closely spaced stations possess less independent information than isolated stations, a factor that must be taken into account when calculating aggregate properties (mean, median, and percentage of significant values across all stations). The individual contribution of each station to the total spatial degrees of freedom was estimated by applying the eigenvector (EOF) method described by Bretherton *et al.* [1999] to concatenated T_s and T_a time series in a two-step process. The first step applied the EOF method to a combination of time series of isolated stations and regional averages (e.g.,

Table 6. Correlations Between Snow Cover Anomaly and Temperature Anomalies

	Surface		Free Air		Delta-T	
	Max	Min	Max	Min	Max	Min
Mean correlation	-0.168	-0.151	-0.152	-0.149	-0.105	-0.043
Median correlation	-0.165	-0.137	-0.131	-0.126	-0.132	-0.058
Mean (abs value)	0.171	0.155	0.156	0.154	0.129	0.064
Max correlation (+ve)	0.083	0.078	0.088	0.095	0.217	0.143
Min correlation (-ve)	-0.547	-0.541	-0.447	-0.455	-0.524	-0.335
Number sig. ^a %	65.0	51.4	73.1	61.2	53.4	19.2
Number m.sig. ^b %	4.4	23.7	2.6	16.9	2.7	8.9
Sig. +ve, %	0	0	0	0	2.4	1.9
Sig. -ve, %	65.0	51.4	73.1	61.2	41.0	17.3
Total -, %	95.7	95.2	93.8	93.1	69.1	74.3

^aSig. means $p < 0.05$ (significant).

^bM.sig. means $p < 0.10$ (marginally significant).

Correlation with Total Cloud Cover

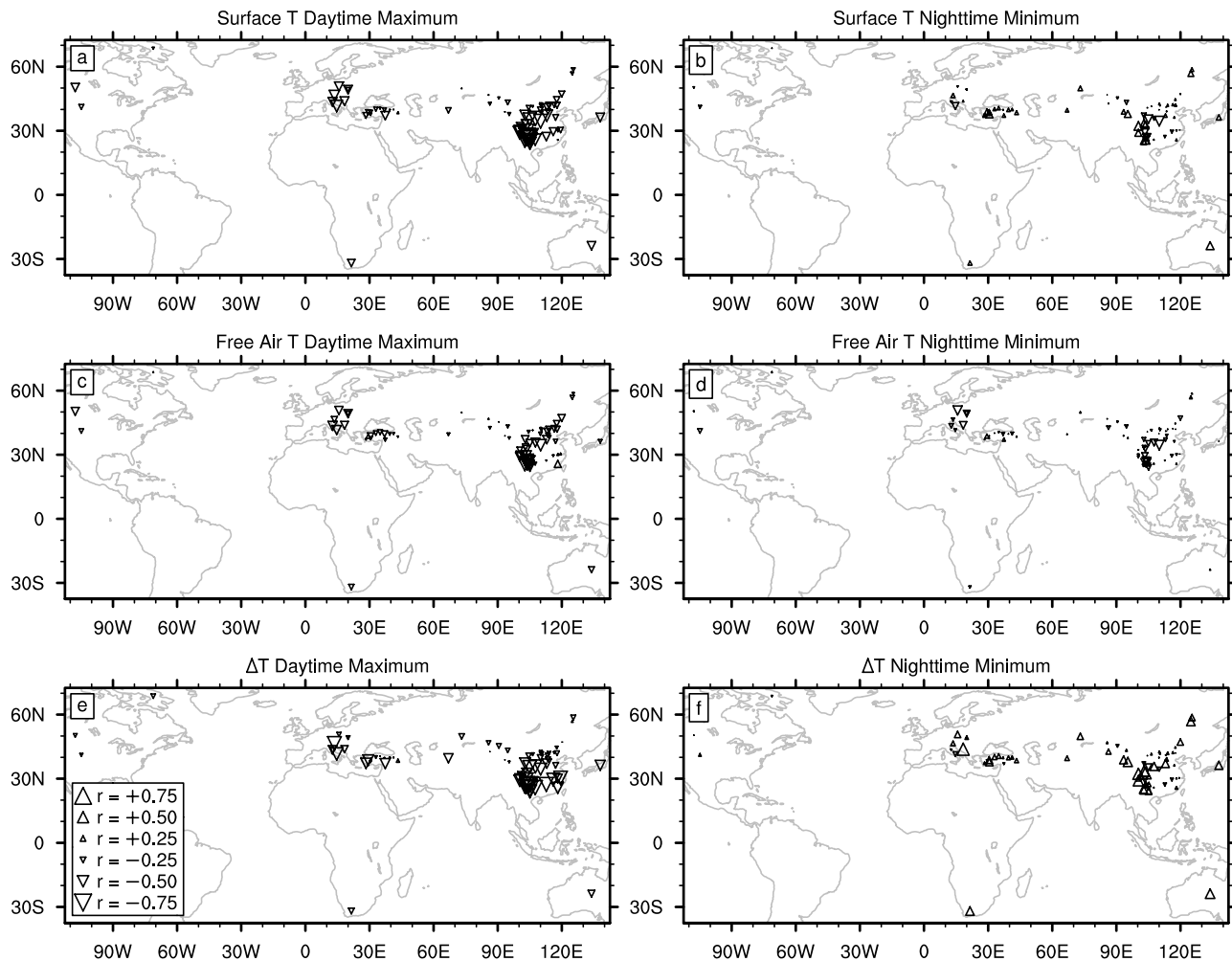


Figure 2. Maps of positive (upward pointing triangle) and negative (downward pointing triangle) correlations between anomalies in temperature and total cloud cover. (a) Surface maximum temperatures, (b) surface minimum temperatures, (c) free-air maximum temperatures, (d) free-air minimum temperatures, (e) ΔT maximum, and (f) ΔT minimum. Triangle size is proportional to correlation magnitude.

Europe, Turkey, China, etc.) to determine which single stations or groups of stations were independent from all of the others. The second step applied the EOF method to each group of stations to determine the spatial degrees of freedom of that group. Individual stations were assigned an effective sample size equal to the number of spatial degrees of freedom in the group divided by the number of stations in the group (last column of Table 1). Values ranged from 1.0 (Australia, South Africa, Baffin Island) to 0.07 (China), and the total effective sample size of all 72 stations was 13.

4. Results

4.1. Correlations

[23] With 5 time periods (4 seasons and all months together), 6 predictands, and 6 controlling variables (2 cloud, 3 wind and 1 snow) for 72 stations, the total number of correlations calculated was 12,960. Thus, of necessity,

only a brief outline of the salient details is discussed. In the summary Tables 2–6 the arithmetic mean correlation can be rather meaningless because of the additive effect of strong negative and positive correlations, so the mean absolute correlation value (ignoring signs) is also given, along with the median value (more robust to outliers). All values are weighted by individual station effective sample size to account for spatial autocorrelation. In this and subsequent tables and figures max(imum) refers to daytime and min(imum) to nighttime. Although for some variables we have an a priori expectation that the correlation has a particular sign (e.g., cloud and snow), statistically significant correlations with the opposite sign can occur because there is a third parameter, such as advection, strongly controlling both such that expected relationship between them is overwhelmed.

4.1.1. Temperatures and Cloud Cover

[24] Table 2 summarizes annual correlations between surface, free-air and ΔT temperatures, and total cloud cover

Correlation with U Wind Component

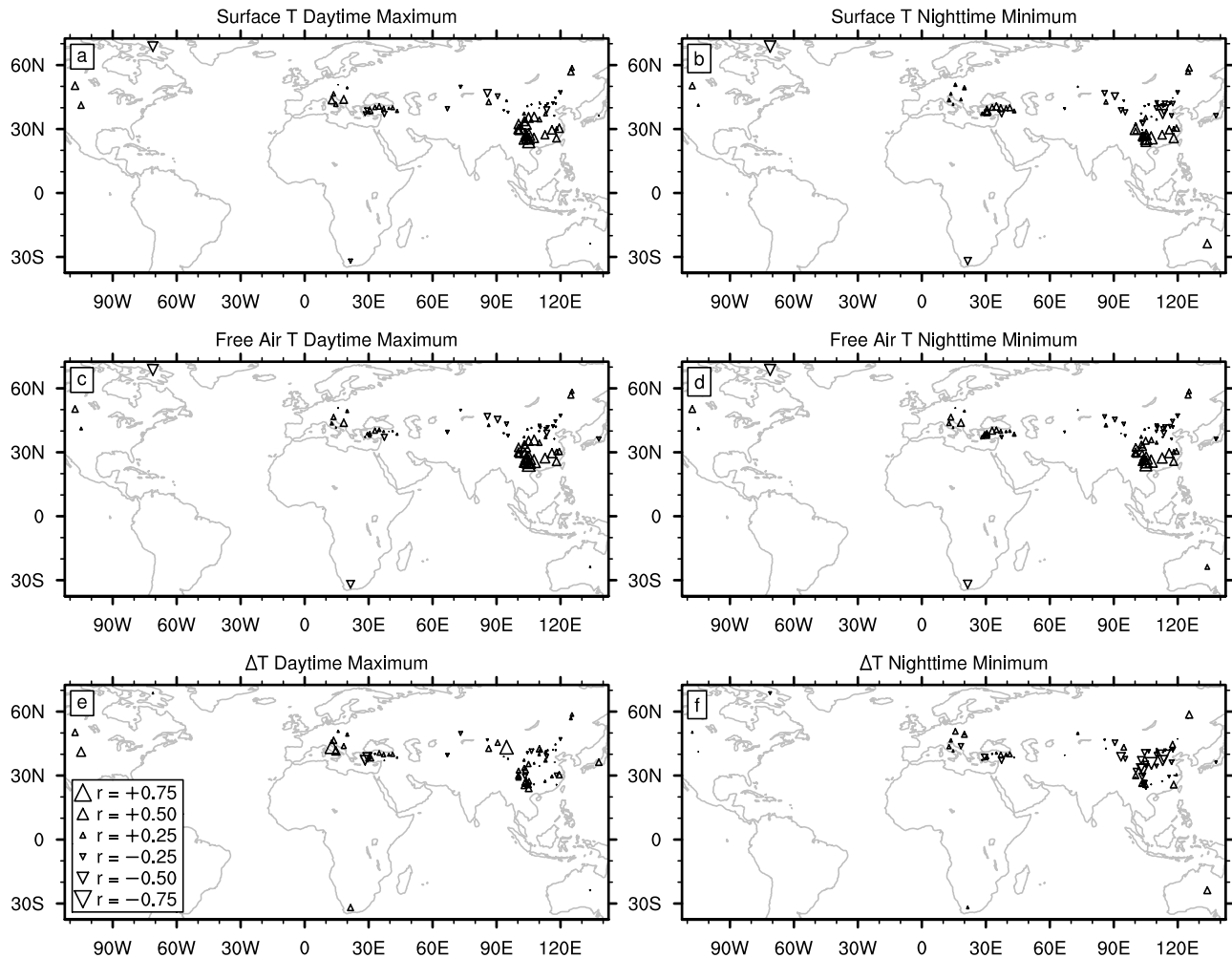


Figure 3. (a–f) As in Figure 2 but for correlations between anomalies in temperature and u wind component.

anomalies. Most sites show significant correlations ($p < 0.05$). Mean and median correlations are usually quite similar. As expected, cloud cover is associated with lower surface maxima and higher surface minima at most sites. The nighttime cloud warming influence is absent in the “free-air” temperatures where the mean correlation is weakly negative. This is confirmed by the strong relationships between ΔT and cloud cover anomalies at most stations, negative by day (more cloud causes surface cooling relative to free air) and positive by night (more cloud leads to surface warming relative to free air). Nighttime correlations between surface and ΔT temperatures and cloud cover anomalies are also strong using low clouds only, since low clouds emit more radiation downward (bottom line of Table 2).

[25] Stations near to one another usually show similar correlations, but much variability occurs at larger scales, suggestive of a regional climate effect (Figure 2). Anomalous stations occasionally occur, but many of these can be explained with some knowledge of local climate. For example, stations with weak correlations between surface maximum temperature and total cloud cover occur mostly in northern and western China (e.g., Hoboksar, Baytik-Shan)

where incursions of cold air from the Siberian high in winter bring bitterly cold but cloud-free conditions even in the daytime (Figure 2a). On the other hand, the strongest negative relationships (below -0.5) center on 30°N and 105°E (Sichuan and Shaanxi provinces) [see Yu *et al.*, 2004]. The daytime cloud/temperature correlation weakens with increasing latitude (metacorrelation $r = 0.451$), consistent with a more prominent cloud cooling effect at lower latitudes due to higher mean sun angle and the counter-influence of daytime cooling under clear skies in winter at higher latitudes (polar air masses). Correlations also become slightly stronger at higher elevations, presumably because of stronger radiative forcing and dependence of surface heating on direct radiation.

[26] In the free air both nighttime and daytime cloud/temperature correlations are stronger at the higher-elevation sites in Europe and Southern China (Figures 2c and 2d). Both the day and night ΔT /cloud correlations (Figures 2e and 2f) are also stronger at the higher-elevation sites in southern China, emphasizing the increased importance of cloud cover at high elevations in preventing rapid relative surface cooling through efficient radiation transfer.

Correlation with V Wind Component

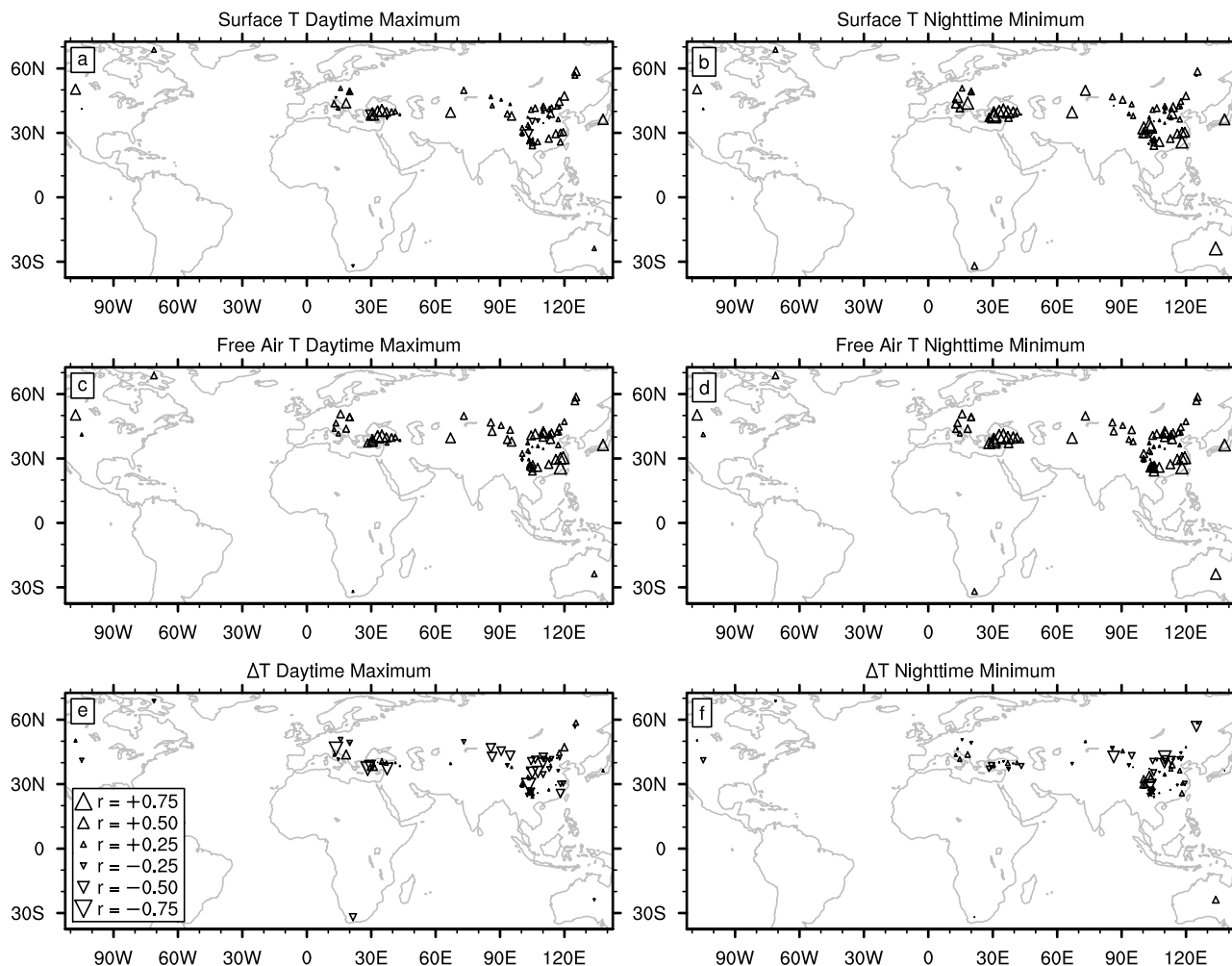


Figure 4. (a–f) As in Figure 2 but for correlations between anomalies in temperature and v wind component.

[27] The fact that significant relationships between total cloud cover anomalies, surface, free-air and ΔT temperatures occur at most sites increases our confidence in the quality of surface and free-air temperature data sets, especially since the cloud data are independent of both.

4.1.2. Temperatures and Regional Wind Components

[28] Tables 3 and 4 provide summaries of the station correlations between temperature anomalies and reanalysis u and v wind component anomalies, respectively.

[29] The relationships with the u wind component are inconsistent and often weak, especially at night, since the characteristics of westerly advection depend on the upstream surface (i.e., factors such as continentality and relief). The relationships between u , surface, free-air temperatures and ΔT are mapped in Figure 3. Increased westerly advection causes surface and free-air warming at more than half the stations, but there are also stations with strong negative correlations (approximately 25% of sites (Table 3)). Over most of Europe an increase in u is associated with increase in surface maxima, while in Asia positive/negative relationships are concentrated in the

south/north of the continent. A broadly similar pattern is seen for surface minima, and for free air temperatures. The big positive correlations between u and surface/free-air temperatures in southern China occur east of the Tibetan Plateau, suggestive of a downslope warming effect. Stronger zonal flow (high u) is associated with a sharpened meridional temperature gradient in China, both at the surface and in the free air. Relationships with ΔT are less consistent.

[30] The v wind component represents meridional advection and exhibits consistent correlations with temperature anomalies. Surface and free-air temperatures are nearly always significantly positively correlated with the v wind component (positive defined as poleward flow) during both day and night (Table 4). Although we may expect that relationships between wind components and free-air temperatures will be stronger than those with surface temperatures because of their common source in the reanalysis, free-air temperatures additionally represent smoothed large-scale anomalies that are less influenced by local radiative effects (aspect, exposure, patterns of cloud formation). The relationship between v and ΔT is usually negative during the

Correlation with Snow Cover

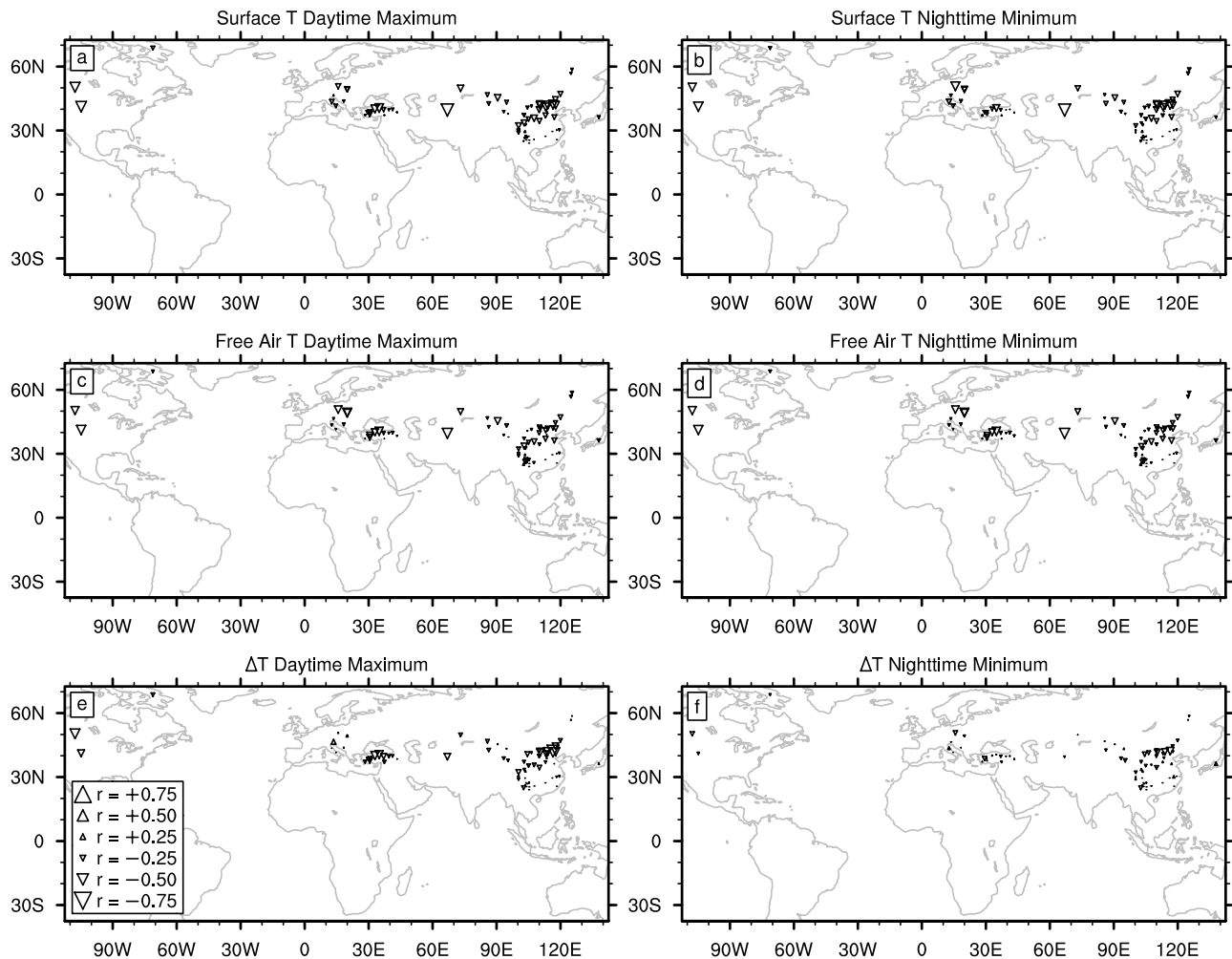


Figure 5. (a–f) As in Figure 2 but for correlations between anomalies in temperature and snow cover.

day (over 60% of stations). Under cold advection in polar air masses (negative v), ΔT is usually high (warm surface in comparison with free air); implying subdued and lagged cooling of the surface. Surface heating similarly lags under warm advection (positive v and low ΔT).

[31] Figure 4 displays spatial maps of the correlations between the v wind component and temperature anomalies. Surface maximum temperatures (Figure 4a) are strongly influenced by v where outbreaks of polar air masses are strong. The few stations with apparently anomalous relationships (negative) include Huajialing, Xifengzhen and Emei in the Sichuan Basin in China. This particular area has a distinct microclimate [Arakawa, 1969; Zhang and Lin, 1992], being protected from incursions of polar air from the north by mountain ranges. Additional downslope warming under northerly winds creates the unusual situation of northerly air masses being warmer than southerly ones at these stations. Other anomalous stations such as Gaziantep in Turkey (37.1°N, 37.4°E, 855 m) and Fraserburg in South Africa (31.9°S, 21.5°E, 1300 m) are prone to downslope winds in equatorward airstreams. The anomalous behavior of Emei (29.5°N, 103.3°E, 3049 m) remains in the map for surface minimum temperatures (Figure 4b), but disappears in the free-air temperature maps (Figures 4c and 4d). The

Table 7. Effect of Seasonal Division on Mean Correlation Strength Between Temperature and Total Cloud/Wind Component Anomalies

Predictors	Predictand					
	Surface		Free Air		Delta-T	
	Max	Min	Max	Min	Max	Min
Total cloud						
Annual	-0.281	0.079	-0.207	-0.065	-0.248	0.179
MAM	-0.286	0.051	-0.215	-0.107	-0.281	0.222
JJA	-0.451	0.017	-0.381	-0.179	-0.261	0.266
SON	-0.383	0.050	-0.279	-0.108	-0.319	0.214
DJF	-0.149	0.112	-0.086	-0.012	-0.178	0.096
U wind						
Annual	0.083	0.054	0.046	0.059	0.136	0.037
MAM	0.031	-0.004	0.021	0.022	0.079	-0.038
JJA	-0.020	-0.074	-0.050	-0.080	0.071	0.071
SON	0.049	-0.009	0.002	0.052	0.134	-0.004
DJF	0.178	0.142	0.128	0.146	0.202	0.089
V wind						
Annual	0.185	0.301	0.265	0.327	-0.086	-0.013
MAM	0.163	0.147	0.201	0.197	-0.041	-0.123
JJA	0.082	0.114	0.112	0.140	-0.016	-0.073
SON	0.155	0.187	0.236	0.259	-0.050	-0.055
DJF	0.249	0.190	0.299	0.259	-0.013	-0.050

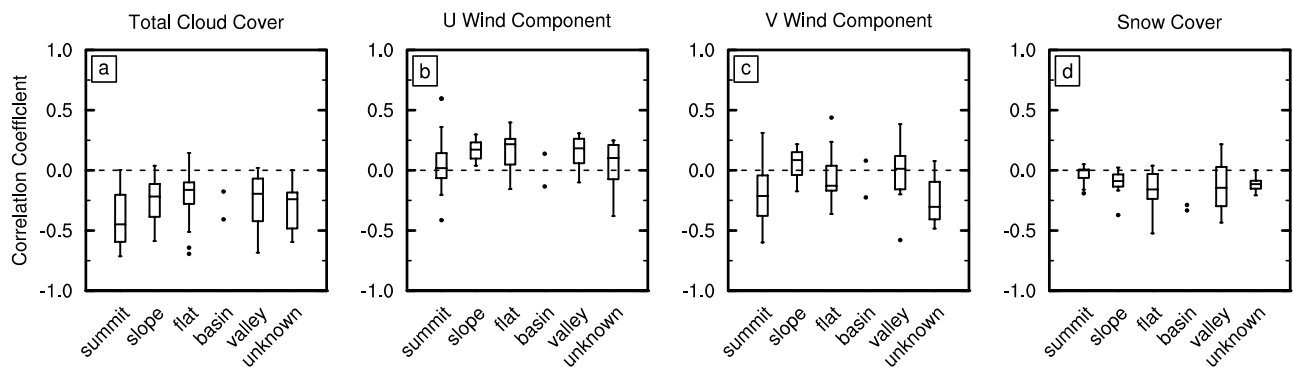
Distribution of Correlation with ΔT Maximum According to Site Topography

Figure 6. Boxplots showing for each topographic class the distribution of correlations between anomalies in ΔT maximum and (a) total cloud cover, (b) u wind component (no significant differences), (c) v wind component, and (d) snow cover. Boxes span the distance between first and third quartiles (the interquartile range, IQR), and the middle line marks the median. Whiskers extend out to the greatest value less than $1.5 \times$ IQR beyond the first and third quartiles, and points mark outliers.

reanalysis behavior is thus decoupled from the surface at this location.

[32] The correlations between ΔT and v exhibit much more variability (Figures 4e and 4f). In most areas poleward advection (high positive v) leads to a heat deficit on the mountain surface (western Europe, southern Turkey, most of northern China) but a minority of stations show the opposite relationship (e.g., Arxan, Xi-Ujimqin-Qi).

4.1.3. Temperatures and Local Wind Speed

[33] The relationships between local wind speed and temperatures are variable (Table 5) and usually only significant at about half the stations (maps not shown). Although correlations with surface and free-air temperatures are often weak, in many cases relationships with ΔT are much stronger. The surface often becomes warmer in comparison with the free air under conditions of strong ventilation. Thus stronger winds make an already negative ΔT less negative at night. Some of the explanation for the weaker correlations may be because the local wind speed observation is highly variable with time and possibly unrepresentative of a long time period.

4.1.4. Temperatures and Snow Cover

[34] Table 6 and Figure 5 present correlations for the 64 out of 72 sites that experienced snow cover. At most locations the correlations between snow cover anomalies and temperature anomalies are significantly negative, albeit relatively weak. For example, the weighted mean correlation for surface temperature during daytime is -0.168 . Correlations tend to be stronger than this in areas where snow cover is sporadic and hence interannual variability is high (e.g., central North America, south central Asia, eastern China around 40°N). Contrastingly, sites in high northern latitudes experiencing extensive snow cover every winter exhibit weakly negative correlations. Correlations with surface temperature are slightly weaker during nighttime than daytime. During the day, correlations with free-air temperatures are slightly weaker than those with surface temperatures. This means that there is a weak negative relationship between daytime ΔT and snow cover at most locations, again strongest in the zone of greatest snow cover variability (Figures 5e and 5f).

4.1.5. General Comments

[35] In conclusion, relationships between temperatures, cloud cover, local wind speed, and snow cover tend to be strongest at the surface, while those with the regional wind components tend to be strongest in the free air. This produces significant relationships between ΔT and cloud, wind, and snow parameters at most stations, the predominant signs of which agree with those expected from consideration of past studies (section 2). However, it is easy to oversimplify our findings. Although significant correlations exist at many stations, the sign of the relationship varies according to location, meaning that the mean absolute correlation value is often higher than the arithmetic mean correlation. Thus any prediction of ΔT must be locally based, and is dependent on local and regional climate.

4.2. Effect of Seasonal Breakdown

[36] Most correlations, especially those with cloud cover (being related to the radiation flux), are seasonally dependent, and subdividing by season often improves

Table 8. Metacorrelations Between Spatial Patterns of Meteorological Parameter/Temperature Correlation Magnitudes For Different Time Periods

	Surface		Free Air		Delta-T	
	Max	Min	Max	Min	Max	Min
<i>1971–1978 (Presatellite) Versus 1979–1996 (Satellite)</i>						
Total cloud	0.795	0.788	0.715	0.632	0.850	0.807
Low cloud	0.769	0.705	0.718	0.622	0.768	0.722
U wind	0.821	0.857	0.838	0.837	0.586	0.783
V wind	0.742	0.835	0.638	0.739	0.734	0.696
Wind speed	0.624	0.437	0.536	0.093	0.745	0.561
Snow	0.637	0.523	0.586	0.569	0.423	0.238
<i>1979–1987 Versus 1988–1996 (Within Satellite Era)</i>						
Total cloud	0.684	0.613	0.764	0.629	0.742	0.569
Low cloud	0.699	0.591	0.812	0.699	0.629	0.599
U wind	0.740	0.733	0.884	0.844	0.556	0.723
V wind	0.673	0.751	0.880	0.889	0.573	0.518
Wind speed	0.432	0.252	0.699	0.535	0.545	0.471
Snow	0.232	0.274	0.354	0.416	0.251	0.126

Table 9. Summary of Forward Stepwise Regression Models to Predict Surface Temperature, Free-Air Temperature and ΔT Anomalies From Six Parameters (Total Cloud, Low Cloud, u and v Wind Components, Local Wind Speed and Snow Cover Anomalies)^a

All Sites	Mean r^2		Number of Times the Predictor Appears in Models With +/- Coefficient					
			Cloud		Wind		Wind Speed	Snow
	All Sites	Elev > 2000 m	Total	Low Only	V Wind	U Wind		
Surface	0.298	0.387	1/46	5/34	52/2	38/15	9/13	1/42
Max temp			97.9	87.2	96.3	71.7	59.1	97.7
Surface	0.258	0.259	15/14	21/4	55/1	27/25	9/7	0/32
Min temp			51.7	84.0	98.2	51.9	56.3	100.0
Free air	0.283	0.264	4/47	8/34	65/0	32/16	5/26	2/45
Max temp			92.2	81.0	100.0	66.7	83.9	95.7
Free air	0.251	0.161	8/31	15/20	68/0	35/18	8/13	0/45
Min temp			79.5	57.1	100.0	66.0	61.9	100.0
ΔT (day)	0.235	0.302	0/37	4/36	11/25	29/8	27/8	2/29
			100.0	90.0	69.4	78.4	77.1	93.5
ΔT (night)	0.167	0.280	28/6	29/4	11/27	15/22	16/9	3/21
			82.4	87.9	71.1	59.5	64.0	87.5

^aVariables have to have p value of less than 0.1 to enter the model. Numbers in the second row are coefficient consistency factors, calculated by (n/t) where n = frequency of most common coefficient sign and t = total number of times the predictor appears. Values above 90% are in bold. Mean r^2 values take spatial autocorrelation into account.

Fractional Variance Explained by Best-Fit Annual Model

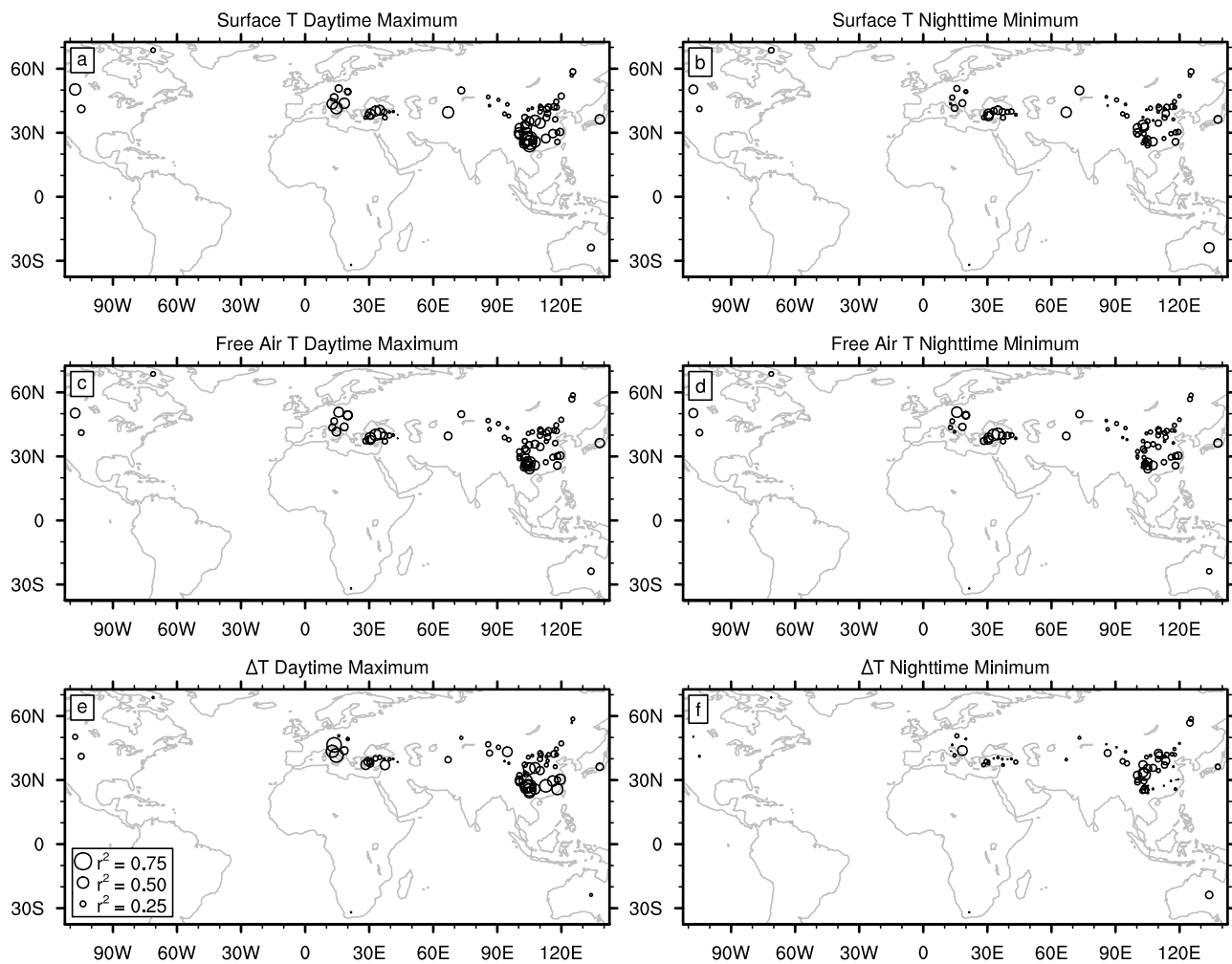


Figure 7. Maps of variance explained (r^2) by stepwise regression model. (a) Surface maximum temperatures, (b) surface minimum temperatures, (c) free-air maximum temperatures, (d) free-air minimum temperatures, (e) ΔT maximum, and (f) ΔT minimum.

Average Fractional Variance Explained by Model For Each Season

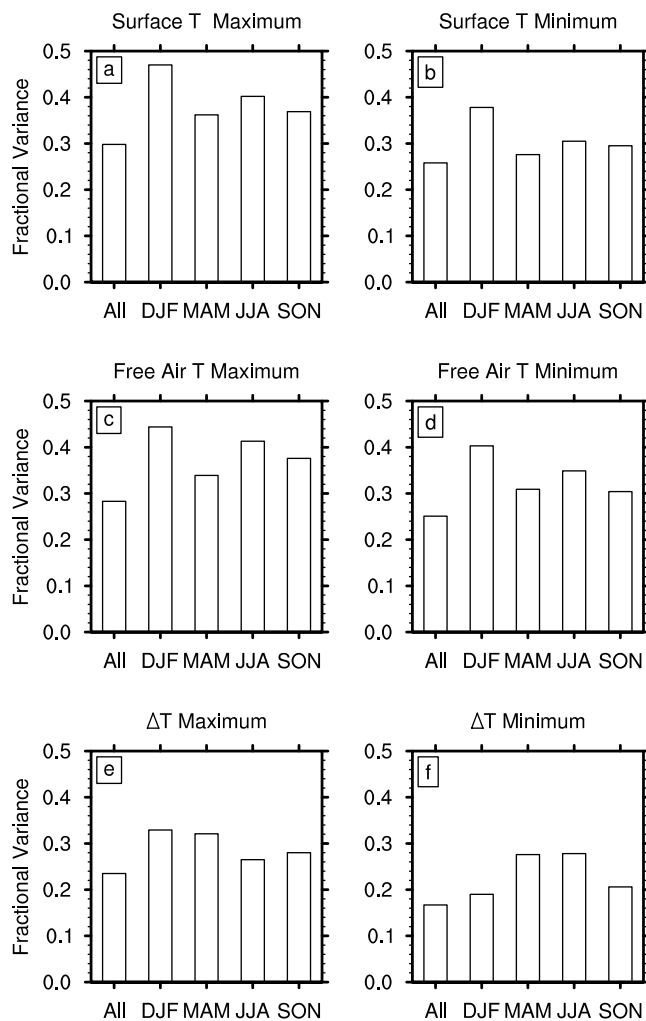


Figure 8. Average fractional variance explained (r^2) by models for all months and individual 3-month seasons. Values are corrected for spatial autocorrelation.

mean values. Table 7 shows mean seasonal correlation values for select predictors (total cloud cover, u and v wind components). Correlations for individual seasons are on average higher than ones for all months, but this is not always the case. Cloud correlations are best in summer because of greater insolation, while wind correlations are better in winter because of greater air mass contrasts. The majority of climates represented are strongly seasonal, particularly in Eurasia where the contrast between northerly and southerly monsoon regimes is distinct.

4.3. Effect of Topography

[37] Each of the 72 sites was classified according to topography using a subjective definition derived from investigation of topographical charts. This is a local definition based on the 5–10 km scale. Because we only selected sites higher than the mean of the surrounding reanalysis grid points, mountain summit sites are fre-

quent. The six classes (numbers of sites in parentheses) included 1: summit or ridge (23), 2: slope (7), 3: flat (15), 4: basin (2), 5: incised valley (16), 6: not enough information to classify because of confusion over exact location or poor mapping (9). Analysis of variance was applied to assess whether topographic class influences correlation magnitudes. Significant differences between classes often occurred, particularly for the mountain summit class. Figure 6 displays box plots for correlations between daytime ΔT and total cloud (Figure 6a), u wind component (no significant differences between classes) (Figure 6b), v wind component (Figure 6c), and snow cover (Figure 6d). The mountain summit class shows stronger cloud cover and v wind component correlations than every other known category, but weaker snow cover correlations than other classes. The flat, basin and valley sites show the opposite. Snow cover not surprisingly has more control over temperatures at basin and valley sites where sky-view factors are lower and surface effects will be more important.

4.4. Effect of Time Period

[38] There is concern that the introduction of satellite data in 1979 had a nonstationary influence on reanalysis temperatures [Sturaro, 2003]. Thus correlations of monthly temperature anomalies with each parameter were calculated for all sites for the separate periods 1971–1978 (presatellite) and 1979–1996 (satellite). Differences in correlation values between the two periods were small and usually insignificant (nearly always less than 0.1 (figures not shown)). Spatial patterns of correlations were compared for the two periods, and also for the subperiods 1979–1987 and 1988–1996 (both during the satellite era). Interestingly, the spatial correlation patterns for ΔT were more different between the two subperiods within the satellite era than between 1971–1978 and 1979–1996 (Table 8). Thus any reanalysis inhomogeneity has had less impact on correlations than internal changes within the satellite era. Overall persistence in correlation patterns is high, suggesting that most relationships are stationary (temporally consistent). The consequences of this are discussed further in section 5. Relationships with snow were the least temporally consistent, possibly because of limited snow extent in the later period.

4.5. Stepwise Regression Models

[39] Forward stepwise regression was employed for surface, free-air temperatures, and ΔT (day and night) at each of the 72 stations with six predictor variables: total and low cloud cover, u and v wind components, local wind speed, and snow cover. A significance of $p = 0.1$ was required for entry into the model (432 models for each season or annual). Table 9 summarizes model performance for the annual case. The first two columns show the mean overall r^2 for the best annual model for all stations and for stations above 2000 m (adjusted for spatial autocorrelation). The other columns give the number of times each predictor was considered significant in the final model, listing the number of times the coefficient for that predictor was positive/negative. Coefficient consistency factors show whether the sign of a predictor coefficient is consistent. If this factor is high (bold >90%) then there is confidence

Trend in Original Temperature

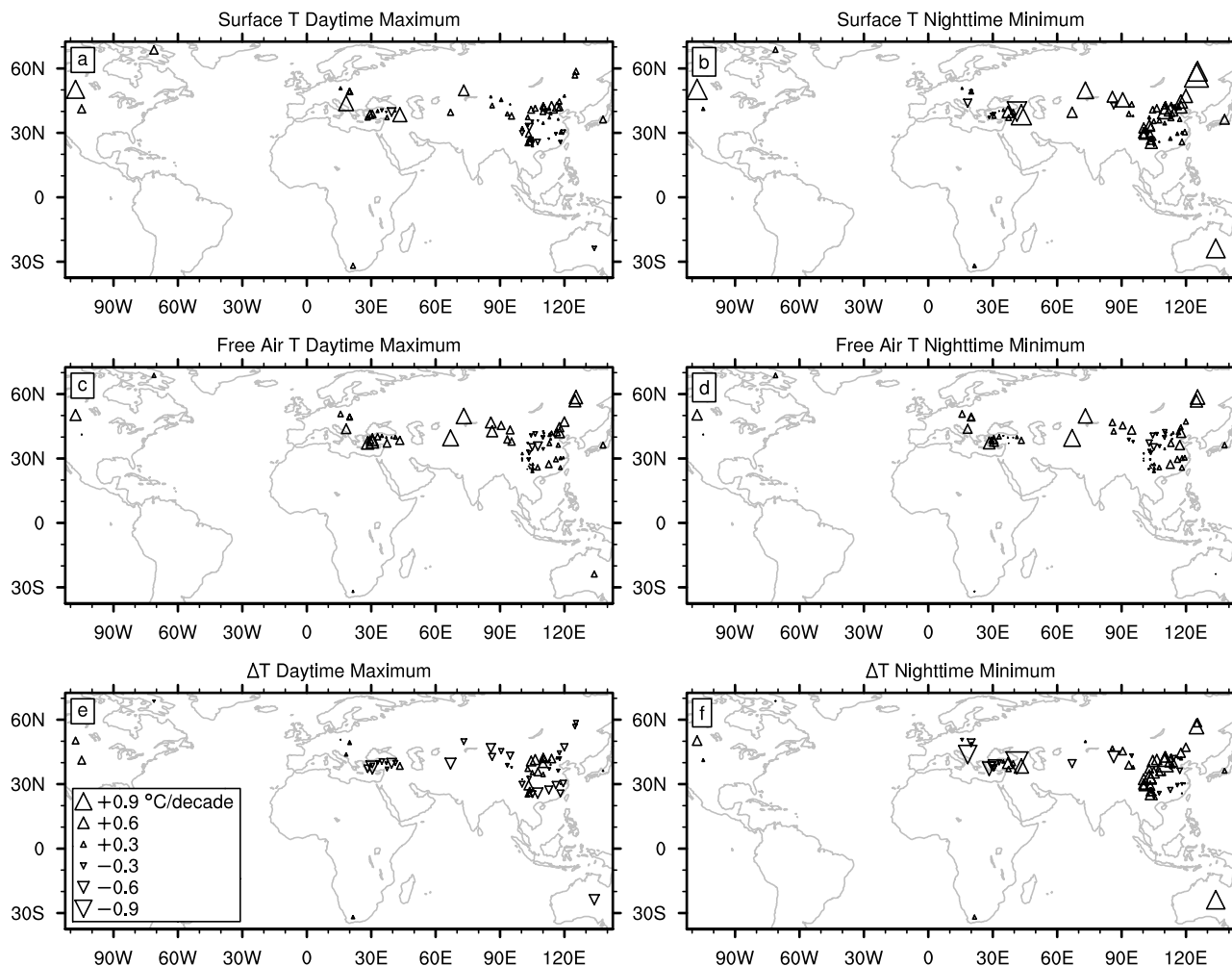


Figure 9. Maps of original surface, free-air and ΔT trends for the 69 stations. (a) Surface maximum temperatures, (b) surface minimum temperatures, (c) free-air maximum temperatures, (d) free-air minimum temperatures, (e) ΔT maximum, and (f) ΔT minimum.

that the effect is real (rather than influenced by multicollinearity between predictors).

[40] Total cloud cover has a consistent cooling effect by day (for surface, free air and ΔT) and the v wind

component and snow cover are consistent for surface and free-air temperatures (but slightly less so for ΔT). Other predictors are often less consistent, especially the u wind component and local wind speed. Although there

Table 10. Surface Temperature, Free-Air Temperature and ΔT Trends for 69 Global Stations Using Monthly Anomalies (1971–1990)^a

	Surface		Free Air		Delta-T	
	Max	Min	Max	Min	Max	Min
Mean trend	0.25 ± 0.16	0.43 ± 0.25	0.29 ± 0.12	0.23 ± 0.12	-0.05 ± 0.12	0.21 ± 0.20
Max trend	0.95	1.27	0.84	0.89	0.52	0.98
Min trend	-0.44	-1.03	-0.44	-0.34	-0.68	-1.16
Median	0.27	0.26	0.28	0.23	-0.09	0.16
U. quartile	0.42	0.75	0.49	0.43	0.16	0.50
L. quartile	0.11	0.16	0.08	0.01	-0.26	-0.04
n	69	69	69	69	69	69
Number +ve, %	77.0	88.1	91.9	77.9	42.9	70.4
Number -ve, %	23.0	11.9	8.1	22.1	57.1	29.6
Number sig. ^b , %	3.6	41.3	27.1	21.2	35.7	53.4
Sig. +ve, %	3.0	41.3	26.0	20.6	14.6	40.8
Sig. -ve, %	0.6	0	1.1	0.6	21.1	12.6

^aTrends are presented in degC/decade, and mean/median values take spatial autocorrelation into account. Errors for the mean trend are based on a 95% confidence interval.

^bSignificant means $p < 0.05$.

Table 11. Summary of Trends in Cloud, Wind and Snow Cover Anomalies, 1971–1990, 69 Global Stations (per Decade)^a

Variable	Daytime Clouds, % cover/decade		Nighttime Clouds, % cover/decade	
	Total	Low	Total	Low
Mean trend	1.84	1.87	2.01	2.33
Median trend	-0.21	-0.56	0.39	0.28
n	69	69	69	69
Number +ve, %	40.2	41.8	54.5	52.7
Number -ve, %	59.8	58.2	45.5	47.3
Number sig., ^b %	39.8	39.1	33.1	37.8
Sig. +ve, %	17.5	29.5	16.9	26.8
Sig. -ve, %	22.3	9.6	16.2	11.0

Variable	Reanalysis Winds, (m/s)/decade		Surface Winds, (m/s)/decade		Snow Anomaly
	V Wind	U Wind	Day Wind Speed	Night Wind Speed	
Mean trend	-0.09	0.02	-0.17	-0.12	-0.020
Median trend	-0.05	0.04	-0.12	-0.04	-0.008
n	69	69	69	69	61 ^c
Number +ve, %	45.5	55.5	34.4	36.6	28.1
Number -ve, %	54.5	44.5	65.6	63.4	71.9
Number sig., ^b %	36.4	38.3	26.2	28.3	36.7
Sig. +ve, %	10.4	24.3	1.8	4.5	5.3
Sig. -ve, %	26.0	14.0	24.4	23.8	31.4

^aMeans and medians take spatial autocorrelation into account.

^bSignificant means $p < 0.05$.

^cEight stations have no (or extremely minimal) snow cover recorded.

Trend in Predicted Temperature

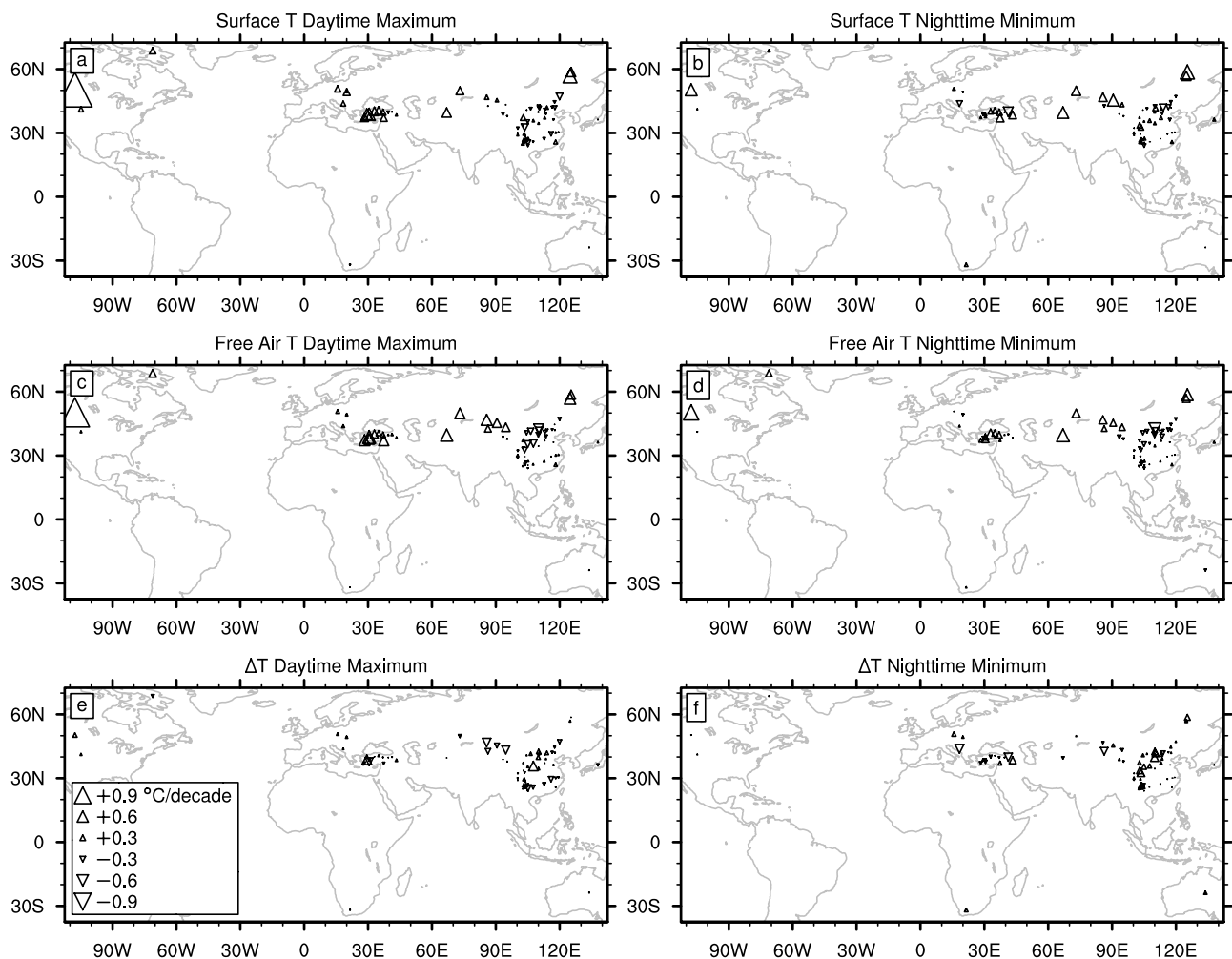


Figure 10. As in Figure 9 but for predicted trends.

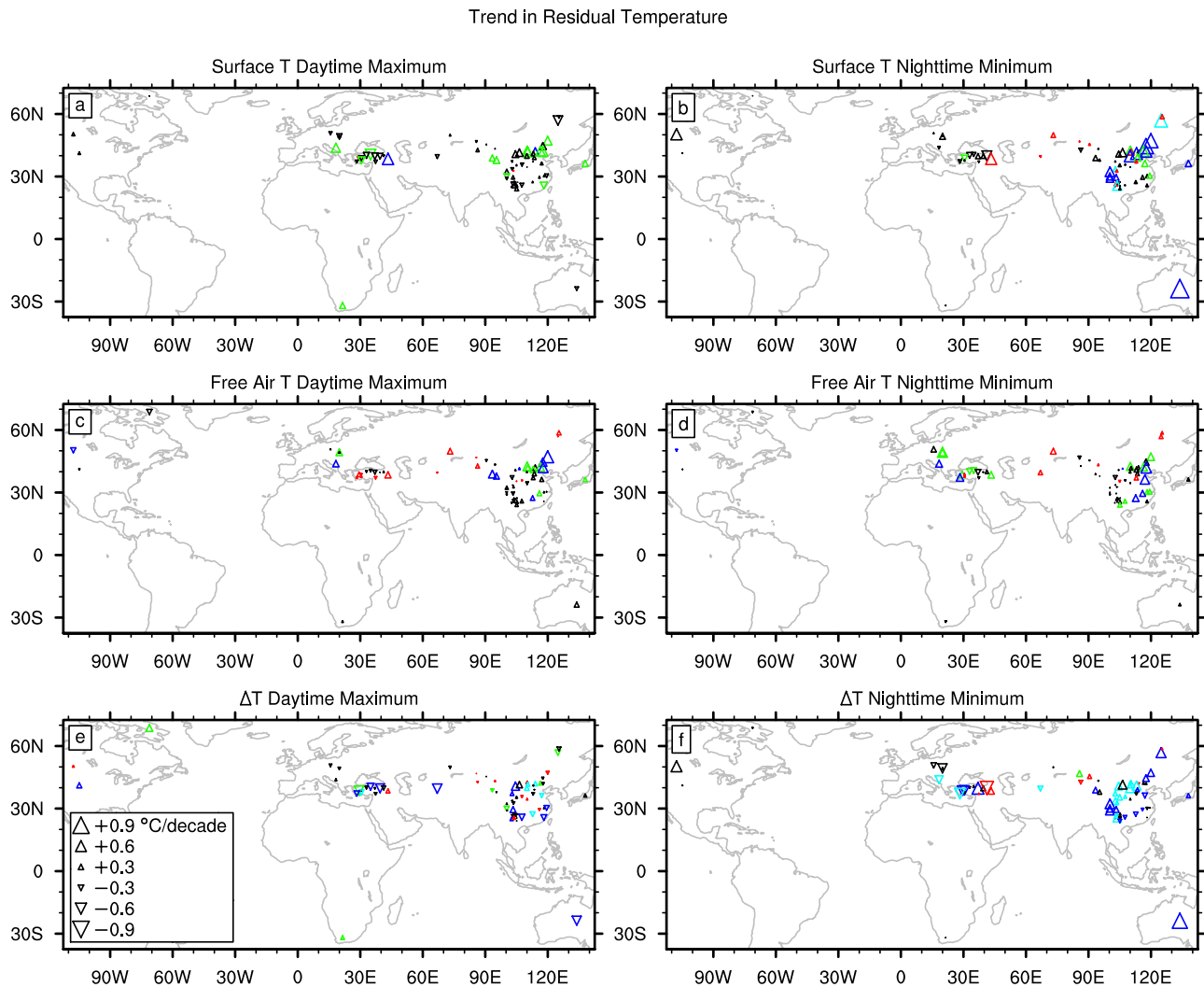


Figure 11. As in Figure 9 but for residual trends. Type A stations are cyan, types B and D are red, type C is blue, types E and G are green, and types F and H are black (see Table 12 and text for definitions).

were strong individual correlations at some stations (>0.7) the mean percentage of temperature variation explained among all stations varies from 16 to 30%. For surface maxima, approximately a third of stations have r^2 above 0.4 and the mean r^2 is 0.30. The mean r^2 is slightly lower for ΔT than for surface or free-air temperatures but higher at sites above 2000 m above sea level.

[41] The spatial variation in annual model r^2 is shown in Figures 7a–7f for the six predictands. Surface maxima are most successfully modeled in North America, Europe and southern China. Surface minima are also modeled well in the same areas. The worst areas for free-air models are in northern and western China centered on Xinjiang province during the day (e.g., Balguntay, Yiwu) and also Sichuan province at night (e.g., Daocheng, Emei Shan). In contrast with the surface models, free-air model performance deteriorates with elevation, especially by night (metacorrelation $r = -0.368$, $p = 0.002$). ΔT models show different patterns with the worst models being much more widely scattered. The best daytime models are in southern China and Europe ($r^2 > 0.5$). Nighttime ΔT r^2 values improve with elevation (metacorrelation $r = 0.460$, $p = 0.0001$) and

show a different distribution. The best predictions are in Northern and Central China, while Turkey and southeastern China show poorer performance (e.g., Tianmu Shan, Nanyue).

[42] Models developed for individual seasons tended to increase r^2 (Figure 8), particularly in winter when the wind variables were useful predictors, and in summer when total cloud cover was a useful predictor. On average there is an increase of approximately 0.1 in mean model r^2 (above the annual models), and the number of station models with $r^2 > 0.5$ increases dramatically. Winter improvements are especially successful, when variable snow cover and wind components (advection) are both important. Nevertheless in the majority of cases at least half of the temperature variability remains unexplained by meteorology.

5. Observed Trends in Temperatures and Other Parameters

[43] Temporal trends in T_s , T_a and ΔT and their controlling parameters were measured by least squares linear

Table 12. Frequencies of Type A–H Stations^a

Type	Significance	Surface		Free Air		Delta-T	
		Max	Min	Max	Min	Max	Min
A	OPR	0	3	0	0	7	16
B	OP	2	9	12	8	10	8
C	OR	2	11	7	6	13	20
D	O	0	2	2	1	0	0
E	PR	4	0	2	3	1	1
F	P	10	11	11	13	8	6
G	R	11	7	5	10	6	0
H	none	40	26	30	28	24	18
Total		69	69	69	69	69	69

^aThe second column shows the combination of trends that is significant. O, original; P, predicted; R, residual. For a detailed definition of categories see the main text.

regression. Significance is assessed using the method of *Santer et al.* [2000], taking temporal autocorrelation into account. 3 stations had too many data gaps to calculate reliable trends and were excluded from further analysis. The original trends themselves are significantly different from those using a wider range of 1084 stations over a longer period [*Pepin and Seidel*, 2005]. However, the purpose here is not to be globally comprehensive but to examine the relationships between T_s , T_a and ΔT trends and simultaneous changes in cloud, wind and snow, where reliable data are available.

5.1. Surface, Free-Air and ΔT Trends: 1971–1990

[44] Maps of T_s , T_a and ΔT trend magnitudes are shown in Figure 9, and aggregate properties with weighting by station effective sample size are listed in Table 10. Many trends are insignificant (Table 10), particularly those for daytime T_s . Quoted errors for the mean trends in Table 10 are based on a 95% confidence interval. During the day, surface trends are not systematically greater than or less than free-air trends, and negative ΔT trends are just as frequent as positive ΔT trends. The mean trend (all stations) for daytime ΔT is not significantly different from zero. Contrastingly, surface warming at night (Figure 9b) exceeds free-air warming (Figure 9d) at most stations, so the trend in ΔT is often positive (mean of $+0.21 \pm 0.2$ °C/decade). Comparison of our T_s and T_a trends with the Northern Hemisphere figures reported by *Fu et al.* [2004] shows strong similarities on a diurnal mean basis, but further discussion of these figures is not advised since our study is not global, and examines a different time period.

5.2. Cloud, Wind and Snow Trends: 1971–1990

[45] Table 11 summarizes trends in nontemperature variables. Cloud cover trends are significant at slightly less than half of sites but trends of both signs are common. There are significant decreases in wind components, local wind speeds, and snow cover at around a quarter of sites.

5.3. Relationships Between Temperature Trends and Trends in Cloud, Wind and Snow

[46] To examine whether the temperature trends in Figure 9 are accounted for by attendant changes in cloud, wind and snow, the original trends (their magnitude and

significance) were compared with trends predicted by the stepwise regression model (predicted trends) and trends in the residual differences between actual and predicted anomalies (residual trends). The predicted trends represent what would result if temperature trends were determined solely by meteorological factors. Note that observational uncertainty in the data will reduce the magnitude of calculated regression coefficients, thus leading to potential underestimation of the predicted trends. The residual trend is the component of temperature change unconnected to changes in meteorology, and NOT the difference between original and predicted trends. Because seasonal models were more successful than annual models, fits and residuals were derived for each season separately using the most appropriate model for that season, and then combined into one long time series. The geographical distribution of predicted and residual trends is shown in Figures 10 and 11 respectively (see Figure 9 for the original trends).

[47] Eight classes of response can be identified, depending on which combination of original [O], predicted [P] and residual [R] trends is significant (Table 12). Only the first four types of response have actual significant observed trends and the other response types (E–H) are of limited interest for the purposes of this study.

[48] Type A stations have significant original, predicted and residual trends. This means that the observed trend is only partially due to meteorological changes. Type B stations have significant predicted trends but not significant residual trends, meaning that the observed trend can be accounted for by the changes in meteorological factors over the same period. Type C stations have no significant predicted trend and a residual trend remaining. This means that variability in meteorological factors does not account for the observed temperature trend. At type D stations, observed trends are significant, but both predicted and residual trends are insignificant. This is rare.

[49] Note that raw frequencies listed in Table 12 do not represent a global average because of the highly uneven density of stations. Comparison of Figures 9 and 11 indicates that at many sites in North America, Europe and Central Asia (70 – 100°E), daytime ΔT residual trends are either insignificant (types B, H) or much smaller than original ΔT trends. This suggests that differences between trends in daytime surface and free-air temperatures for these high-elevation regions of the globe can largely be explained by changes in meteorological conditions. In parts of Turkey and eastern China, the negative residual daytime ΔT trends could indicate that the strength of the relationship between temperature and cloud cover has changed over time [*Sun et al.*, 2000]. Large increases in anthropogenic aerosols in these two regions may have radiatively cooled or retarded the warming of the surface relative to the atmosphere [e.g., *Tayanç et al.*, 1997; *Luo et al.*, 2001; *Kaiser and Qian*, 2002; *Che et al.*, 2005], a factor not taken into account in our model. In northern China there are several type A stations where the meteorology only partly accounts for (often positive) ΔT change. Although aerosol loading in China is small north of 40°N [*Luo et al.*, 2001; *Kaiser and Qian*, 2002], the cause of our positive residual daytime ΔT trends in this area is unknown. This may have arisen because of predicted trends being underestimated because of observation uncertainty.

[50] Large nighttime ΔT residual trends are present in many regions of the globe. Positive trends predominate, resulting from greater warming of the surface than the free air. Further investigation into the causes of this contrast is required; speculative reasons include land use change and urbanization. Most of these stations are again sited in China. Type A and C stations are more common than type B, demonstrating that at the majority of locations variance due to meteorology cannot (solely) account for the observed nighttime trends. Such significant nighttime ΔT residual trends could indicate that (1) important parameters are missing from the models that could have accounted for the trends, (2) the residual trends are real and occur over and above meteorological forcing due to other forcing factors (e.g., increasing carbon dioxide concentration or aerosol loading or land use change), or (3) the original trends in ΔT must be spurious because they cannot be explained by meteorology, and therefore result from systematic changes in instrumental errors over time.

[51] It is our feeling that, although r^2 is modest (0.3–0.4) in most models, the most influential controlling meteorological factors (surface controls, advection and radiation balance) have been included, and so inclusion of further variables is unlikely to improve r^2 dramatically. This leaves the latter two interpretations.

6. Summary and Discussion

[52] We have examined the relationships between surface temperatures, free-air temperatures, their difference (ΔT), and meteorological parameters (cloud, wind and snow cover) for 72 exposed high-elevation stations with reliable observations. Significant, but subtly different, relationships exist at the majority of locations, suggesting that meteorological processes are partially responsible for causing differences between observed surface temperatures (GHCN and CRU) and free-air temperatures (reanalysis R1 interpolated to similar elevations). This implies that the surface and free-air observations are measuring physically different quantities and so should be expected to differ (both in instantaneous values and in trends). The cloud and snow data and some of the wind data (local wind values) are independent of both the surface and free-air temperature data sets, adding more weight to this interpretation.

[53] The signs of the relationships between ΔT and meteorological parameters at the majority of sites are as expected from a consideration of the physical processes involved (outlined in section 2). ΔT becomes more negative under cloudy conditions during the day, but more positive at night (e.g., cloud minimizes the difference in temperature between the surface and the free atmosphere). In most locations, warm advection (positive v) makes ΔT more negative because of the lag effect. Relationships with u are more variable, dependent on regional climatic controls. Relationships with snow cover are usually negative since the snow acts as a heat sink at the surface in comparison to the free atmosphere.

[54] Typically a third to a half of the variance in ΔT on a seasonal basis can be explained by variation in these meteorological parameters. The remaining half or more of the variance could be controlled by unknown parameters or result from instrumental error or sampling problems (for

example, time differences between reanalysis and surface observations, which, although fairly constant at any one location, could have a variable influence on ΔT).

[55] Trends in surface temperature, free-air temperature, and ΔT were shown at many sites. ΔT trends are often significant but inconsistent by day (meaning that the surface is not warming at the same rate as the free air) but positive during the night (meaning enhanced surface warming relative to the free atmosphere). Once observed cloud, wind and snow changes are taken into account, daytime residual temperature trends are small for most stations outside of Turkey and eastern China. Negative daytime residual trends in Turkey and eastern China may result from increased radiative surface cooling by anthropogenic aerosols. Significant nighttime residual trends are more widespread, and only part of the variance in ΔT can be explained through meteorology at these locations since the contrast between measured free-air and surface temperatures is not supported by attendant changes in cloud, wind and snow.

[56] To ensure that predicted trends were independent from trends in the data used to calculate the model coefficients, a similar methodology was applied after detrending all anomalies (temperatures and other parameters) before running the stepwise regression. The detrending had minimal effect on model r^2 or on results in nearly all cases. This confirms that the temperature variance due to meteorology is more or less independent of that due to trends.

[57] A few caveats must be mentioned. The original trends derived using the 69 stations are not necessarily representative of global conditions or longer time periods. Many are in eastern Asia. Indeed they are dissimilar to trends calculated for a larger number of high-elevation stations (1084) over a longer time period (1948–2002) [Pepin and Seidel, 2005] where positive trends in ΔT were predominant. Thus the findings concerning coherence between ΔT trends and controlling parameters should only be extrapolated spatially with extreme care. It would be profitable to expand this type of analysis to longer time periods and more comprehensive data sets, but this requires compatible simultaneous homogenous data for many parameters.

[58] The preceding results indicate that, for many regions, differences in daytime maximum temperature trends measured at high-elevation stations and in the free atmosphere primarily result from changes in cloud cover, wind, and snow. Where this is not the case, there have been large increases in anthropogenic aerosols over the past several decades. Attribution of differences in nighttime minimum temperature trends is uncertain and may indicate the occurrence of unaccounted meteorological changes or presence of inhomogeneities in the data. Since the reanalysis is a mixture of free-air data (satellite and radiosonde), it is not possible to expand these findings here to discuss differences between individual free-air and surface data sets such as LKS [Lanzante *et al.*, 2003] and/or MSU2 [Mears *et al.*, 2003; Vinnikov and Grody, 2003; Fu *et al.*, 2004] versus CRU [Jones and Moberg, 2003]. A similar analysis relating such inter-data-set differences to other atmospheric variables would be a useful, but difficult, exercise mainly because of problems in ensuring temporal and spatial consistency in comparisons. Nevertheless the use of other variables (cloud, wind, surface properties,

atmospheric moisture etc) to help examine the validity of inter-data-set temperature differences deserves further consideration.

[59] **Acknowledgments.** The majority of this work was undertaken while N. Pepin was a visiting scientist at the NOAA Air Resources Laboratory in Silver Spring, MD. Funding was provided by the National Research Council of the United States of America. J. Norris was supported by an NSF CAREER award, ATM02-38527. The helpful guidance of Dian Seidel and the Climate Variability and Trends Group is appreciated.

References

- Arakawa, H. (Ed.) (1969), *Climates of Northern and Eastern Asia*, vol. 8, *World Survey of Climatology*, Elsevier, New York.
- Armstrong, R. L., and M. J. Brodzik (2002), *Northern Hemisphere EASE-Grid Weekly Snow Cover and Sea Ice Extent Version 2* [CD-ROM], Natl. Snow and Ice Data Cent., Boulder, Colo.
- Barry, R. G. (1992), *Mountain Weather and Climate*, 2nd ed., 402 pp., Routledge, Boca Raton, Fla.
- Bretherton, C. S., M. Wildmann, V. P. Dymnikov, J. M. Wallace, and I. Bladé (1999), The effective number of spatial degrees of freedom in a time-varying field, *J. Clim.*, *12*, 1990–2009.
- Che, H. Z., G. Y. Shi, X. Y. Zhang, R. Arimoto, J. Q. Zhao, L. Xu, B. Wang, and Z. H. Chen (2005), Analysis of 40 years of solar radiation data from China, 1961–2000, *Geophys. Res. Lett.*, *32*, L06803, doi:10.1029/2004GL022322.
- Chelliah, M., and C. F. Ropelewski (2000), Reanalysis-based tropospheric temperature estimates: Uncertainties in the context of global climate change detection, *J. Clim.*, *13*, 3187–3205.
- Christy, J. R., et al. (2003), Error estimates of version 5.0 of MSU-AMSU bulk atmospheric temperatures, *J. Atmos. Oceanic Technol.*, *20*, 613–629.
- Fu, Q., C. M. Johanson, S. G. Warren, and D. J. Seidel (2004), Contribution of stratospheric cooling to satellite-inferred tropospheric temperature trends, *Nature*, *429*, 55–58.
- Hahn, C. J., and S. G. Warren (1999), Extended edited synoptic cloud reports from ships and land stations over the globe, 1952–1996, *Numer. Data Package NDP-026C*, Carbon Dioxide Inf. Anal. Cent., Oak Ridge Natl. Lab., Oak Ridge, Tenn.
- Hahn, C. J., S. G. Warren, and J. London (1995), The effect of moonlight on observation of cloud cover at night, and application to cloud climatology, *J. Clim.*, *8*, 1429–1446.
- Jones, P. D. (1994), Hemispheric surface air temperature variations: A reanalysis and update to 1993, *J. Clim.*, *7*, 1794–1802.
- Jones, P. D., and A. Moberg (2003), Hemispheric and large-scale surface air temperature variations: An extensive revision and an update to 2001, *J. Clim.*, *10*, 206–223.
- Jones, P. D., M. New, D. E. Parker, S. Martin, and I. G. Rigor (1999), Surface air temperature and its changes over the past 150 years, *Rev. Geophys.*, *37*, 173–199.
- Kaiser, D. P., and Y. Qian (2002), Decreasing trends in sunshine duration over China for 1954–1998: Indication of increased haze pollution?, *Geophys. Res. Lett.*, *29*(21), 2042, doi:10.1029/2002GL016057.
- Kalnay, E., and M. Cai (2003), Impact of urbanization and land-use change on climate, *Nature*, *423*, 528–531.
- Kanamitsu, M., W. Ebisuzaki, J. Woolen, J. Potter, and M. Fiorino (2002), NCEP/DOE AMIP-II Reanalysis (R-2), *Bull. Am. Meteorol. Soc.*, *83*, 1631–1643.
- Kistler, R., et al. (2001), The NCEP/NCAR 50-year reanalysis, *Bull. Am. Meteorol. Soc.*, *82*, 247–268.
- Lanzante, J. R., S. A. Klein, and D. J. Seidel (2003), Temporal homogenization of monthly radiosonde temperature data, *J. Clim.*, *16*, 224–262.
- Luo, Y., D. Lu, X. Zhou, W. Li, and Q. He (2001), Characteristics of the spatial distribution and year variation of aerosol optical depth over China in last 30 years, *J. Geophys. Res.*, *106*, 14,501–14,513.
- McCutchan, M. H. (1983), Comparing temperature and humidity on a mountain slope and in the free-air nearby, *Mon. Weather Rev.*, *111*, 836–845.
- Mears, C. A., M. C. Schabel, and F. J. Wentz (2003), A reanalysis of the MSU channel 2 tropospheric temperature record, *J. Clim.*, *16*, 3650–3664.
- Molnar, P., and K. Emanuel (1999), Temperature profiles in radiative-convective equilibrium above surfaces at different heights, *J. Geophys. Res.*, *104*, 24,265–24,271.
- National Research Council (2000), *Reconciling Observations of Global Temperature Change*, 85 pp., Natl. Acad. Press, Washington, D. C.
- Pepin, N. C., and M. L. Losleben (2002), Climate change in the Colorado Rocky Mountains: Free-air versus surface temperature trends, *Int. J. Climatol.*, *22*, 311–329.
- Pepin, N. C., and D. J. Seidel (2005), A global comparison of surface and free-air temperatures at high elevations, *J. Geophys. Res.*, *110*, D03104, doi:10.1029/2004JD005047.
- Peterson, T. C., and R. S. Vose (1997), An overview of the Global Historical Climatology Network temperature database, *Bull. Am. Meteorol. Soc.*, *78*, 2837–2848.
- Peterson, T. C., et al. (1998), Homogeneity adjustments of in situ atmospheric climate data: A review, *Int. J. Climatol.*, *18*, 1493–1517.
- Richner, H., and P. D. Phillips (1984), A comparison of temperatures from mountain-tops and the free-atmosphere—Their diurnal variation and mean difference, *Mon. Weather Rev.*, *112*, 1328–1340.
- Samson, C. A. (1965), A comparison of mountain slope and radiosonde observations, *Mon. Weather Rev.*, *93*, 327–330.
- Santer, B. D., T. M. L. Wigley, J. S. Boyle, D. J. Gaffen, J. J. Hnilo, D. Nychka, D. E. Parker, and K. E. Taylor (2000), Statistical significance of trends and trend differences in layer-average atmospheric time series, *J. Geophys. Res.*, *105*, 7337–7356.
- Seidel, D. J., and M. Free (2003), Comparison of lower-tropospheric temperature climatologies and trends at low and high elevation radiosonde sites, *Clim. Change*, *59*, 53–74.
- Sturaro, G. (2003), A closer look at the climatological discontinuities present in the NCEP/NCAR reanalysis temperature due to the introduction of satellite data, *Clim. Dyn.*, *21*, 309–316.
- Sun, B., P. Y. Groisman, R. S. Bradley, and F. T. Keimig (2000), Temporal changes in the observed relationship between cloud cover and surface air temperature, *J. Clim.*, *13*, 4341–4357.
- Tabony, R. C. (1985), The variation of surface temperature with altitude, *Meteorol. Mag.*, *114*, 37–48.
- Tayanç, M., M. Karaca, and O. Yenigün (1997), Annual and seasonal air temperature trend patterns of climate change and urbanization effects in relation to air pollutants in Turkey, *J. Geophys. Res.*, *102*, 1909–1919.
- Trenberth, K. (2004), Rural land-use change and climate, *Nature*, *427*, 213–214.
- Vinnikov, K. Y., and N. C. Grody (2003), Global warming trend of mean tropospheric temperature observed by satellites, *Science*, *302*, 269–272.
- Vose, R. S., T. R. Karl, D. R. Easterling, C. N. Williams, and M. J. Menne (2004), Impact of land-use change on climate, *Nature*, *427*, 213–214.
- Yu, R., B. Wang, and T. Zhou (2004), Climate effects of the deep continental stratus clouds generated by the Tibetan Plateau, *J. Clim.*, *17*, 2702–2713.
- Zhang, J., and Z. Lin (1992), *Climate of China*, 376 pp., John Wiley, Hoboken, N. J.

J. R. Norris, Scripps Institution of Oceanography, 9500 Gilman Drive 0224, La Jolla, CA 92093-0224, USA. (jnorris@ucsd.edu)

N. C. Pepin, Department of Geography, Buckingham Building, Lion Terrace, University of Portsmouth, Hants PO1 3HE, UK. (nicholas.pepin@port.ac.uk)